Electronic Supplementary Information

Acridine orange as a coreactant for efficient electrogenerated chemiluminescence of tris(2,2′-bipyridine)ruthenium(II) and its use for selective and sensitive detection of thiourea

Muhammad Saqib[a], Shahida Bashir[b], Shimeles Addisu Kitte[a], Haijuan Li[a], Yongdong Jin[a,c]*

[a]*State Key Laboratory of Electroanalytical Chemistry, Changchun Institute of Applied Chemistry, Chinese Academy of Sciences, 5625 Renmin Street, Changchun, Jilin 130022, P. R. China*

[b] *Faculty of Science, Department of Mathematics, University of Gujrat, Gujrat 50700, Pakistan*

[c] *University of Science and Technology of China, Hefei 230026, P. R. China*

Corresponding Author

* Tel: +86-431-85262661. Fax: +86-431-85262661.

E-mail: ydjin@ciac.ac.cn.

Table of Contents

1. Experimental section

1.1 Chemicals and materials

Tripropylamine (TPrA), glucose (Glu), tris(2,2'-bipyridyl)dichlororuthenium(II) hexahydrate ($Ru(bpy)_3Cl_2 \cdot 6H_2O$), uric acid (UA), and ascorbic acid (AA) were bought from Sigma–Aldrich (USA). Superoxide dismutase (SOD), glutathione (GSH), acridine orange hemi(zinc chloride) salt (AO), and dopamine (DA) were obtained from Aladdin Reagent Co., Ltd. (Shanghai, China). Sodium sulfite (SS) and thiourea (ThU) were purchased from Alfa Aesar Chemical Reagent Co., Ltd. (China). L-glutamic acid (Glut), aspartic acid (Asp), hydroxylamine (HA), and L-arginine (Arg) were purchased from Shanghai Yuanju Biotechnology Co. Ltd. (Shanghai, China). L-cysteine (Cys), L-tryptophan (Tryp), sodium oxalate ($C_2O_4^{2-}$), urea, and hydroxyurea (HU) were supplied by Sinopharm Chemical Reagent Co. Ltd. (Beijing, China). All the metal salts used in this work were purchased from Beijing Chemical Reagent Company (Beijing, China). The working phosphate buffer solution (pH 7.4, 0.1 M PBS) was prepared by thorough mixing of stock solutions of NaH_2PO_4 and Na_2HPO_4. All the chemicals used in this work were of analytical grade reagents and purified water was obtained using a Millipore system (18.2 MΩ· cm).

1.2 Apparatus

ECL measurements were performed on a multifunctional MPI-A ECL detection system (Xi'An Remex Electronic Science & Technology Co. Ltd., Xi'An, China) in a homemade transparent bottom three-electrode cell. The photomultiplier tube (PMT) of the ECL analyzer was adjusted to achieve optimal intensities. A conventional three-electrode system was applied for the electrochemical and ECL experiments. The working, reference and counter electrodes were glassy carbon electrode (GCE), Ag/AgCl (saturated KCl) and Pt wire electrode, respectively. Differential pulse voltammetry (DPV) was conducted with CHI660E electrochemical workstation (Chenhua, Shanghai). Prior each experiment, GCE was polished with alumina slurry (0.3 and 0.05 μm), cleaned with ultrapure water, and then dried. The anodic ECL was recorded by scanning the electrode potential in the range of 0.2 to 1.25 V with a scan rate of 100 mV/s in 0.1 M PBS solution (pH 7.4). The emission spectrum of the system was recorded in cyclic voltammetry (CV) mode by using a series of wavelength filters (400−700 nm) over PMT of ECL analyzer.

1.3 Procedure of ECL detection of ThU

The ECL detection of ThU on an MPI-A ECL analyzer was performed by immersing the GCE into 600 μl of 0.1 M PBS solution (pH 7.4) with 350 μM of AO and 800 μM of $Ru(bpy)_3^{2+}$, containing various amounts of ThU, respectively. The ECL intensities were recorded by setting the PMT voltage at 700V, potential scan from 0.2 to 1.25 V, and the scan rate at 100 mV/s.

2. Optimization of Detection Conditions

To achieve optimal applicability of the developed ECL system, a set of crucial experiments were performed. As basic environment (pH) might cause negative effects on biomolecules detection, a physiological pH of 7.4 was opted to enhance the applicability of the methods, and the ECL emission at pH 7.4 totally satisfied the detection requirements as well.

It is well known that the ECL emission is highly depended on the concentration of emitter ($Ru(bpy)_3^{2+}$) and coreactant (AO). Therfore, the effect of both $Ru(bpy)_3^{2+}$ and AO concentrations was tested from 25-1666 µM and 5-1600 µM, respectively. As shown in **Fig. S5 & S6**, the ECL signals increase sharply with extension of the concentration up to 800 µM and 350 µM, respectively, and reached a plateau afterwards. Therefore, 0.8 mM of $Ru(bpy)_3^{2+}$ and 0.35 mM of AO were selected as the optimal concentrations for subsequent experiments.

Moreover, the scan rate effect on the ECL intensity and electrooxidation rate of system was further investigated from 5 to 500 mV/s. As shown in **Fig. 3**, the ECL intensity and anodic currents increased linearly with the square root of scan rates ($v^{1/2}$), suggesting that the ECL reaction is diffusion controlled. A scan rate of 0.1 V/s was chosen in the subsequent experiments. In addition, the effect of applied potentail on ECL intensity was also optimized from 0.9-1.5 V. The maximum ECL intensity was achieved at a potential of +1.3 V (**Fig. S7**).

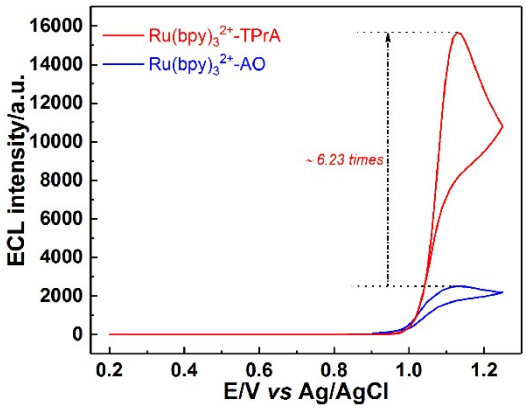

Fig. S1. Comparison of anodic ECL–potential profiles for $Ru(bpy)_3^{2+}$-AO and $Ru(bpy)_3^{2+}$-TPrA. Concentrations: $Ru(bpy)_3^{2+}$: 0.8 mM; AO and TPrA: 0.35 mM; pH: 7.4 (0.1 M PBS); PMT: 700 V

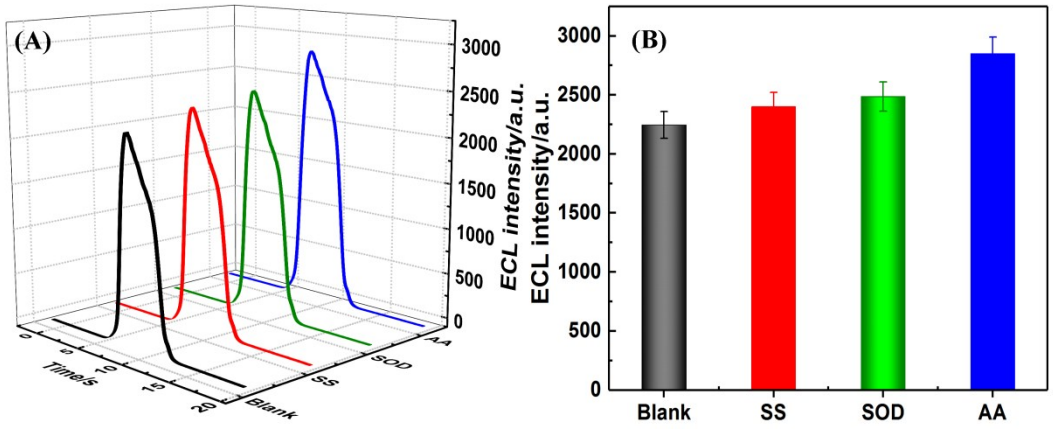

Fig. S2. The effect of radical scavengers on the ECL intensity of $Ru(bpy)_3^{2+}$-AO system. Concentrations: AA (0.50 mM); SS (0.50 mM); SOD (6.0 μg/mL). The experiment was tested at pH 7.4 (0.1 M PBS) in the presence of 0.35 mM AO and 0.8 mM $Ru(bpy)_3^{2+}$ solution; PMT: 700 V.

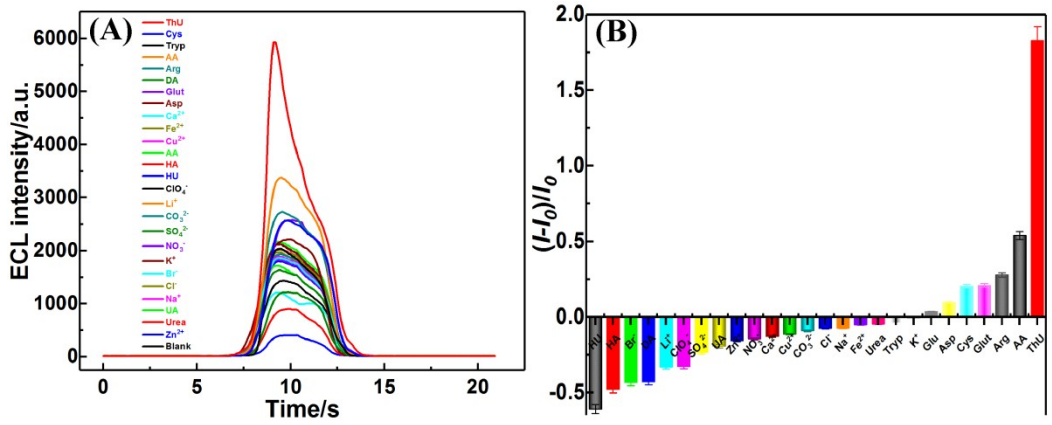

Fig. S3. Selectivity performance of the developed ThU ECL sensing platform. (A) ECL-time profiles for various interferants, and (B) corresponding bar plot for selectivity of the as-developed ECL method. The concentration of all interfering compounds was 10-fold higher (1 mM) than the concentration of ThU (100 µM). The selectivity test was performed at pH 7.4 (0.1 M PBS) in the presence of 0.35 mM AO and 0.8 mM $Ru(bpy)_3^{2+}$ solution; PMT: 700 V.

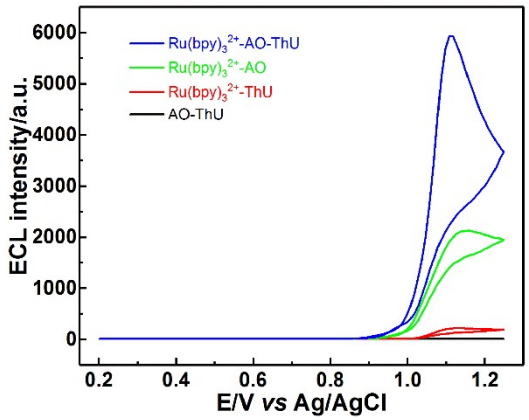

Fig. S4. ECL–potential profiles for the four tested different solutions: AO-ThU (black curve), $Ru(bpy)_3^{2+}$-ThU (red curve), $Ru(bpy)_3^{2+}$-AO (green curve), $Ru(bpy)_3^{2+}$-AO-ThU (blue curve). Concentration of $Ru(bpy)_3^{2+}$ and AO was 0.8 mM and 0.35 mM, respectively; Concentration of ThU: 100 µM; pH: 7.4 (0.1 M PBS); PMT: 700 V.

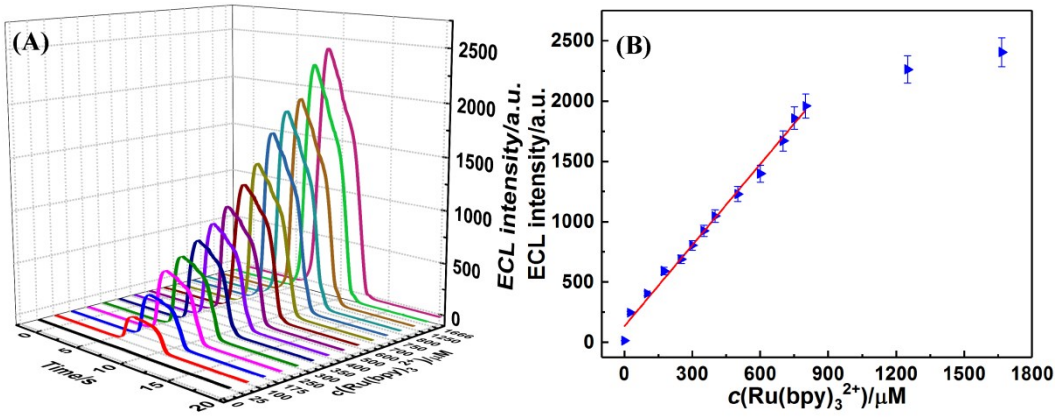

Fig. S5. (A) The effect of $Ru(bpy)_3^{2+}$ concentration on the ECL intensity, and **(B)** corresponding linear relationship between ECL intensity and $Ru(bpy)_3^{2+}$ concentration from 25-800 μM. The experiment was tested at pH 7.4 (0.1 M PBS) in the presence of 0.35 mM AO; PMT: 700 V.

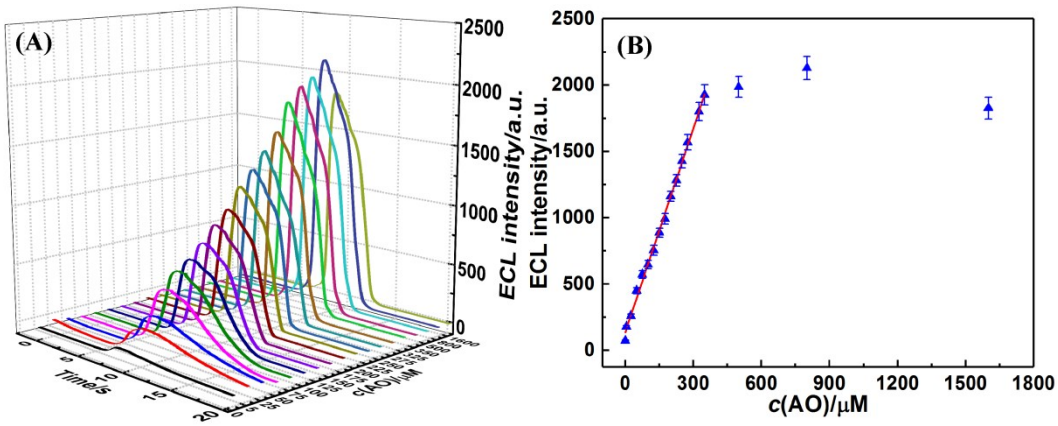

Fig. S6. **(A)** The effect of AO concentration on the ECL intensity, and **(B)** corresponding linear relationship between ECL intensity and AO concentration from 5-350 μM. The experiment was tested at pH 7.4 (0.1 M PBS) in the presence of 0.8 mM $Ru(bpy)_3^{2+}$; PMT: 700 V.

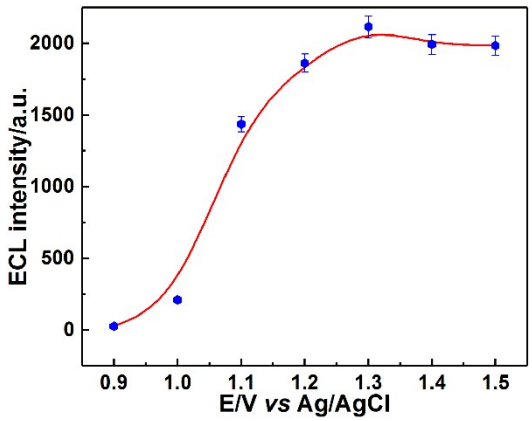

Fig. S7. Effect of applied potential on the ECL intensity of the $Ru(bpy)_3^{2+}$-AO system. The experiment was conducted at pH 7.4 (0.1 M PBS) in the presence of 0.35 mM AO and 0.8 mM $Ru(bpy)_3^{2+}$ solution; PMT: 700 V.

Table S1. Comparison of reported different methods for the detection of ThU

Analytical Method	Probe/Materials	Linear range	LOD	Ref.
Colorimetry	fluorescein and AuNPs	0.05–3.0 μM	0.023 μM	[1]
TRES (chemosensor)	iridium(III) complex	10–200 μM	3.85 μM	[2]
FL	nitrogen doped carbon dots (NCDs)	0.90–10.0 μM	0.15 μM	[3]
FL	nitrogen-doped graphene quantum dots	0.5–14 μM	0.0417 μM	[4]
EIS	nanostructured silver (Nano-Ag) film with carbon paper (CP) substrate (Nano-Ag/CP)	26.3–3284.3 μM	26.3 μM	[5]
CV	manganese oxide nanospheres /deoxyribonucleic (DNA)	50–3000 μM	14 & 22 μM	[6]
CV	graphene nanosheets–Ag nanoparticles	1–3000 μM	0.7 μM	[7]
Amperometry	tin doped manganese dioxide/CNT nanocomposites (Sn MnO_2/CNT)	10–100 μM	0.68 μM	[8]
UV–Vis Spectroscopy	chromogenic probe *N*-chloroacetyl parafuchsin	5.0–0.2 mM	2.1 μM	[9]
UV–Vis Spectroscopy	quinones	97–768 μM	11 μM	[10]
FTIR Spectroscopy	iodine and sodium hydrogen carbonate solutions	77–1016 μM	13 μM	[11]
Kinetic spectrophotometry (catalytic effect)	Janus green (JG) with potassium iodate	0.1–154 μM	0.1 μM	[12]
kinetic spectrophotometry (induction period effect)	meta cresol purple (MCP) with bromate	1.31–78.8 μM	0.26 μM	[13]
Inhibitor biosensor	dissolved oxygen probe	1–20 μM	1.0 μM	[14]
CL	nitrogen-doped carbon quantum dots (NCD)	0.1–10.0 μM	0.038 μM	[15]
HPLC	------	------	0.026 μM	[16]
Mass spectrometry	------	0.13–65.68 μM	0.013 μM	[17]
Raman spectroscopy	------	3.8×10^4–2.6×10^5 μM	------	[18]
ECL	------	0.1–500 μM	10 nM	Present Work

TRES: Time-resolved emission spectroscopy**; FL:** fluorescence**; EIS:** Electrochemical impedance spectroscopy**; CV:** cyclic voltammetry**; UV-Vis:** ultraviolet visible**; FTIR;** Fourier transform infrared resonance**; CL:** chemiluminescence**; HPLC:** high performance liquid chromatography**; ECL:** electrochemiluminescence

Table S2. Detection recoveries of ThU in tap water, orange juice, and orange peel real samples

Samples		Concentrations of ThU (μM)			Recovery (%)	RSD (n=3;%)
		Amount Detected [a]	Amount Added	Amount Found [b]		
ThU	Tap Water	N.D	0.0	---	---	---
			1.0	0.983	98.30	1.88
			5.0	5.11	102.2	2.13
			10.0	10.15	101.5	2.20
	Orange Juice	N.D	0.0	---	---	---
			1.0	0.991	99.10	2.06
			5.0	5.18	103.6	2.19
			10.0	10.42	104.2	2.35
	Orange Peel	0.103	0.0	---	---	2.42
			1.0	1.094	99.18	2.51
			5.0	5.107	100.1	2.36
			10.0	10.31	102.0	2.65

[ab] The average of three replicate determinations. N.D = Not Detected.

References

1. C. Chen, D. Zhao, J. Sun and X. Yang, *Analyst*, 2016, **141**, 2581-2587.
2. W. Wang, Z.-Z. Dong, C. Yang, G. Li, Y.-C. Tse, C.-H. Leung and D.-L. Ma, *Sens. Actuators B*, 2017, **251**, 374-379.
3. C. Zhang, S. Wu, Y. Yu and F. Chen, *Spectrochim. Acta Part A*, 2020, **227**, 117666.
4. X. Fan and Z. Fan, *Anal. Lett.*, 2019, **52**, 2028-2040.
5. S. A. Mozaffari, H. S. Amoli, S. Simorgh and R. Rahmanian, *Electrochim. Acta*, 2015, **184**, 475-482.
6. A. Maleki, H. Daraei and N. Amini, *J. Colloid Interface Sci.*, 2017, **504**, 579-585.
7. A. Safavi, R. Ahmadi, F. A. Mahyari and M. Tohidi, *Sens. Actuators B*, 2015, **207**, 668-672.
8. P. Saharan, A. K. Sharma, V. Kumar and I. Kaushal, *Mater. Chem. Phys.*, 2019, **221**, 239-249.
9. X.-F. Yang and H. Wang, *Spectrochim. Acta Part A*, 2006, **65**, 1063-1068.
10. A. N. de Oliveira, H. de Santana, C. T. B. V. Zaia and D. A. M. Zaia, *J. Food Compos. Anal.*, 2004, **17**, 165-177.
11. K. Kargosha, M. Khanmohammadi and M. Ghadiri, *Analyst*, 2001, **126**, 1432-1435.
12. S. Abbasi, H. Khani, L. Hosseinzadeh and Z. Safari, *J. Hazard. Mater.*, 2010, **174**, 257-262.
13. M. Arab Chamjangali, G. Bagherian, N. Goudarzi and S. Mehrjoo-Irani, *J. Anal. Sci. Technol.*, 2015, **6**, 10.
14. M. K. Sezgintürk and E. Dinçkaya, *Food Bioprocess Technol.*, 2008, **3**, 128.
15. Y. Liu and S. Han, *Food Anal. Methods*, 2017, **10**, 3398-3406.
16. J. Rethmeier, G. Neumann, C. Stumpf, A. Rabenstein and C. Vogt, *J. Chromatogr. A*, 2001, **934**, 129-134.
17. A. Raffaelli, S. Pucci, R. Lazzaroni and P. Salvadori, *Rapid Commun. Mass Spectrom.*, 1997, **11**, 259-264.
18. H. J. Bowley, E. A. Crathorne and D. L. Gerrard, *Analyst*, 1986, **111**, 539-542.